THE ASTROPHYSICAL JOURNAL, 278:575–581, 1984 March 15

STELLAR POPULATIONS IN LOCAL GROUP DWARF ELLIPTICAL GALAXIES. II. NGC 205

JEREMY MOULD
Palomar Observatory;[1] and Kitt Peak National Observatory
JEROME KRISTIAN[2]
Mount Wilson and Las Campanas Observatories,[2] Carnegie Institution of Washington
AND
G. S. DA COSTA[2]
Yale University Observatory
Received 1983 July 22; accepted 1983 August 25

ABSTRACT

We present deep *VRI* photometry from CCD data taken in an off-center field of NGC 205, a dwarf elliptical companion of M31. The color-magnitude diagram shows the bright two magnitudes of the red giant branch, to a magnitude fainter than $I = 22$. Comparison with color-magnitude diagrams of galactic globular clusters and Local Group spheroidal galaxies shows: (1) the metallicity of NGC 205 is at least -0.85 ± 0.2, and it has a real metallicity dispersion of at least 0.5 dex; (2) from the brightness of the tip of the giant branch in NGC 205, its distance modulus is 24.3 ± 0.2 mag, in good agreement with the currently accepted distance modulus for M31; (3) we can set an upper limit of about 10% on the presence of an intermediate-age component in this region of NGC 205. The results for NGC 205 are in general very similar to those of a parallel study of NGC 147, although NGC 205 has a marginally larger metallicity and a larger metallicity dispersion.

Subject headings: galaxies: individual — galaxies: Local Group — galaxies: photometry — galaxies: stellar content

I. INTRODUCTION

NGC 205 is the largest of the four dwarf elliptical companions of M31. It was first resolved into stars by Baade (1944), who subsequently noted the presence of young blue stars near its center (Baade 1951). NGC 205 was classified Epec/S0_1 by Sandage (1961) and has several notable peculiarities. These include distortion of the outer isophotes (Hodge 1973), presumably due to an interaction with M31, conspicuous dust clouds, and the presence of neutral hydrogen (Johnson and Gottesman 1982; see also Unwin 1980). An intermediate-age population in the central parts of NGC 205 has been suggested from photometry by Gallagher and Mould (1981).

The Population I component of NGC 205 is concentrated in the central few hundred parsecs (Hodge 1973), while the present study, which aims to carry out the deepest possible ground-based photometry, is restricted by the available resolution to the outlying regions of the galaxy. This investigation is focused, therefore, on the old stellar population in NGC 205. Deep CCD photometry on the *VRI* system is presented in § II, and the giant branch is compared with those of Galactic globular clusters in § III. The morphology and location of the giant branch allow us in § IV to determine the degree of chemical enrichment in the outer parts of NGC 205 and to set constraints on its stellar population.

[1] Palomar Observatory is operated by the California Institute of Technology.

[2] Visiting Astronomer, Kitt Peak National Observatory, which is operated by AURA, Inc., under contract with the NSF.

II. IMAGING AND PHOTOMETRY

A description of the instrumentation and calibration procedures used in this project was given by Mould, Kristian, and Da Costa (1983, hereafter Paper I). The field chosen for study in NGC 205 was 9'.5 (2 kpc) north of the center, near the major axis. The field lies approximately 11 kpc from the center of M31, close to its minor axis. Data were taken on the nights of 1981 October 30 and November 1, the same nights the NGC 147 data of Paper I were taken. The total exposure times were 40 minutes in *I* and 60 minutes in each of *V* and *R*. To establish the photometric zero points for the subsequent point-spread function (PSF) fitting photometry, a set of 10 reference stars was chosen in the NGC 205 field. These are identified in Figure 1 (Plate 5). Because of the greater crowding in this field, it proved a little harder to calibrate these stars than it did the reference stars in NGC 147. After some experimentation, we adopted the following technique: (1) the intensity of the local reference stars over their central 2" was measured directly on each exposure; (2) this was converted to a total intensity by using the PSF for stars on the frame; (3) this total intensity was compared with total intensity measurements of the primary photometric standards.

The magnitudes obtained in this way (Table 1) have a formal uncertainty of 0.01 mag in $\langle m' - m_R \rangle$ (see Paper I). Results from other calibration techniques, however, suggest that systematic color errors of order 0.03 mag cannot be excluded in the present data.

Photometry of 288 stars in the NGC 205 field is recorded in Table 2. These stars were selected by visual inspection as suitable for accurate photometry. They are identified in

PLATE 5

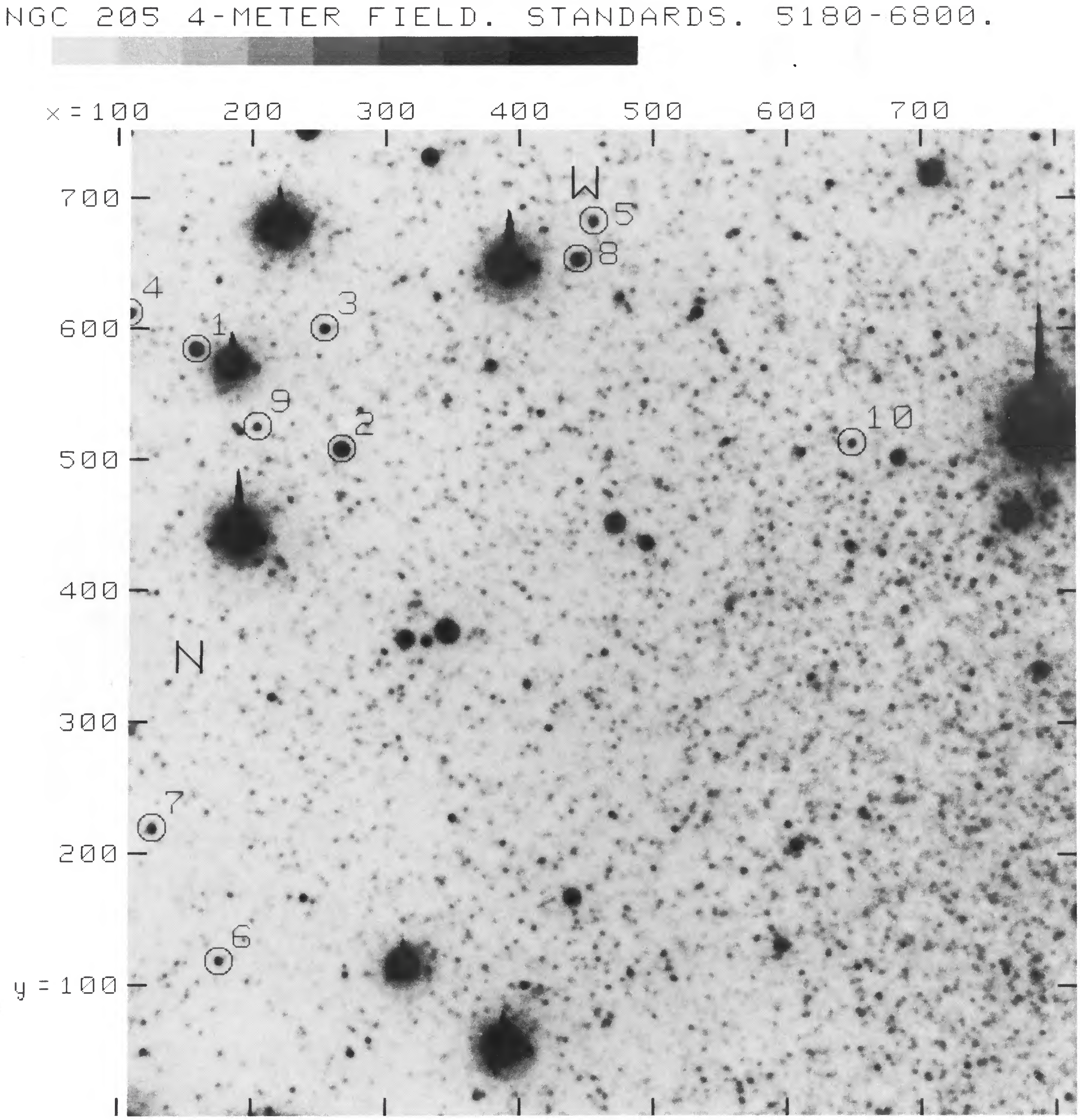

FIG. 1.—The field, in the outskirts of NGC 205, studied in this paper. The values of x and y on the axes are the pixel numbers given in Tables 1 and 2. The numbered stars are the local photometric reference stars listed in Table 1. This picture is a total CCD exposure of 60 minutes in the R band; the limiting magnitude is $R = 23.5$ mag. The size of the field shown is 210″ by 225″.

MOULD, KRISTIAN, AND DA COSTA (*see* page 575)

TABLE 1

APERTURE PHOTOMETRY OF REFERENCE STARS IN NGC 205

No.	V	$V-I$	$V-R$	x	y
1	19.67	2.47	1.16	159	585
2	18.43	1.06	0.46	268	509
3	20.72	2.16	1.02	255	601
4	20.53	2.38	...	108	613
5	21.25	1.79	0.96	456	683
6	20.63	0.86	0.40	177	119
7	21.20[a]	1.75[a]	0.95	127	220
8	19.49	1.72	0.83	444	654
9	21.53	2.16	1.02	205	526
10	20.82	0.79	0.31	649	514

[a] Not included in the fit.

Figure 2 (Plate 6). Columns (2), (4), and (6) give the values of I, $V-R$, and $V-I$ on the Cousins (1976*a*, *b*) system. The associated formal uncertainties in fitting the PSF are listed in columns (3), (5), and (7). A blank in column (5) or (7) where there is an entry for the corresponding color indicates a lower limit on that color. Columns (8) and (9) give the coordinates of these stars to the nearest pixel (0".30 per pixel). The 1950 position of star 12 is $0^h37^m13^s.0$, 41°34′39″.

The degree to which the formal errors in Table 2 underestimate the true photometric uncertainties (due mainly to source confusion) was investigated, as in Paper I, by the addition of artificial stars to the data. At $I = 21.35$ mag, the rms uncertainty in I is 0.24 mag and in $V-I$ is 0.18 mag. The corresponding formal values from 17 stars in Table 2 are 0.06 and 0.10.

The two-color diagram from Table 2 is plotted in Figure 3, together with a mean $(V-I, V-R)$ relation for NGC 147 from Paper I. Since the difference in reddening between the two galaxies is small, their color-color plots are intrinsically similar.

III. THE COLOR-MAGNITUDE DIAGRAM

Figure 4 is the color $(V-I)$–magnitude (I) diagram for NGC 205 from the data of Table 2. It shows the first two magnitudes of the red giant branch in NGC 205. Putting aside for a moment possible contamination of this field by stars in the halo of M31, we can compare Figure 4 with the $(I, V-I)$-diagram for the off-galaxy field in Paper I (Fig. 7 of that paper). It appears that, brighter than about 20th I magnitude, we are seeing field stars. Fainter than 20th magnitude, there is a giant branch with considerable color dispersion.

Quantitative comparison with the giant branches of Galactic globular clusters can be effected, given the distance modulus and reddening. Following the discussion in Paper I, we assume that NGC 205 lies somewhere within 70 kpc of the center of M31, which yields a distance modulus of 24.2 ± 0.3. From the reddening maps of Burstein and Heiles (1982) we assume an extinction of $E(B-V) = 0.06 \pm 0.02$, $E(V-I) = 0.08$, $A_I = 0.11$. The giant branches of M92 and 47 Tuc from Paper I, corrected for this value of the extinction, are superposed on Figure 4. Most of the red giants in NGC 205 lie between the giant branches of M92 and 47 Tuc. But unlike the case of NGC 147 (Paper I, Fig. 6), 47 Tuc does not seem to bound the NGC 205 giant branch on the red side; NGC 205 appears to contain stars of higher metallicity than 47 Tuc.

For a quantitative estimate of the metallicity of stars in this field we follow the recipe of Paper I: estimate the mean

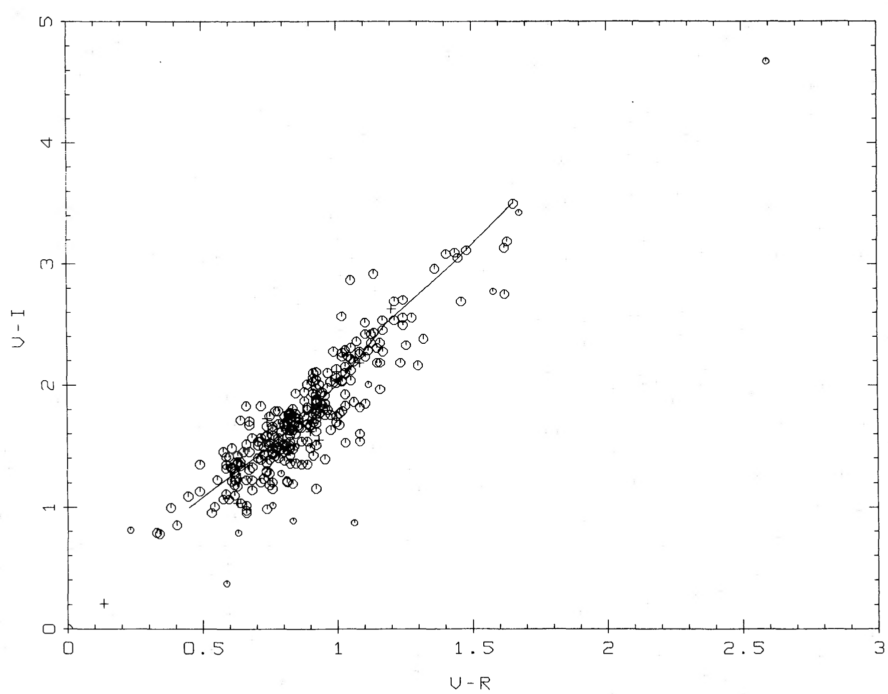

FIG. 3.—The color-color plot for the NGC 205 stars in Table 2. The line is a mean line from a parallel study of NGC 147 (Paper I). The large open symbols record stars with color uncertainties from Table 2 of less than 0.3 mag; for the smaller symbols, the uncertainties are larger than 0.3 mag. The crosses represent lower limits on the measured colors.

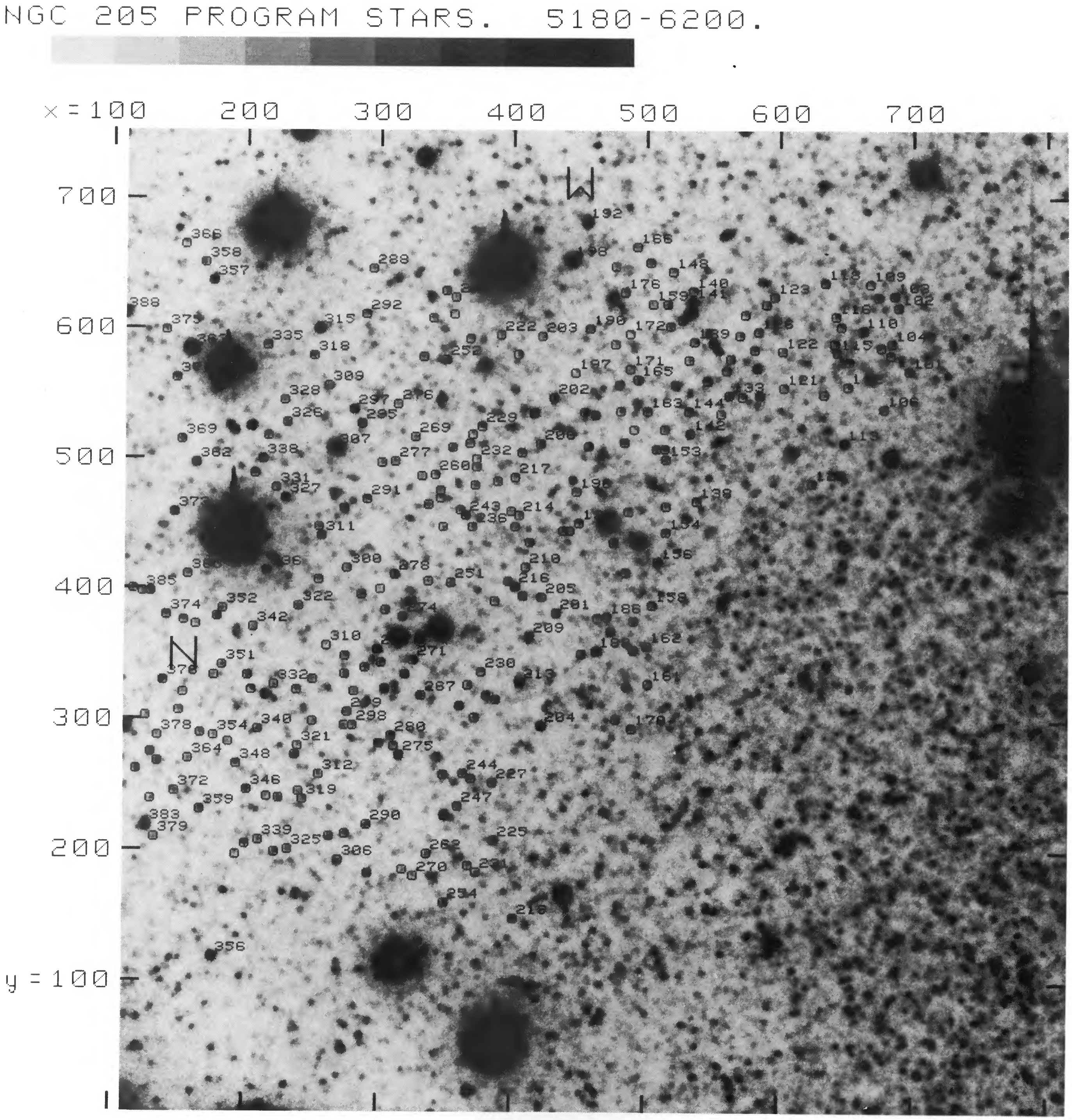

FIG. 2.—An identification chart for the program stars listed in Table 2. All stars are circled, and some of them are labeled with the identifying numbers in col. (1) of Table 2. In order to avoid overlap, not all stars are labeled. The labels are all in the same relative location, above and to the right of the corresponding stars. The x and y pixel locations (cols. [8] and [9] of Table 2) are shown on the axes. The data are the same as in Fig. 1.

MOULD, KRISTIAN, AND DA COSTA (*see* page 576)

TABLE 2

PHOTOMETRY OF STARS IN NGC 205

No. (1)	I (2)	$\pm$[a] (3)	$V-R$ (4)	$\pm$[a] (5)	$V-I$ (6)	$\pm$[a] (7)	x (8)	y (9)
100	20.85	0.03	1.28	0.11	2.55	0.11	707	618
101	21.16	0.05	0.76	0.02	1.44	0.05	697	568
102	21.36	0.04	0.66	0.04	1.52	0.05	689	617
103	20.60	0.01	1.12	0.05	2.28	0.05	686	626
104	20.97	0.03	0.89	0.04	1.80	0.05	684	589
105	20.51	0.02	1.66	0.15	3.50	0.15	683	580
106	21.53	0.10	0.80	0.06	1.66	0.12	678	539
107	21.92	0.12	0.89	0.09	1.35	0.15	676	586
108	21.39	0.07	0.76	0.04	1.43	0.08	674	625
109	22.09	0.26	0.60	0.10	1.07	0.28	668	635
110	20.13	0.01	1.03	0.01	2.10	0.01	662	599
111	20.98	0.07	...	...	1.77	0.07	652	575
112	22.07	0.22	0.62	0.07	1.10	0.23	651	556
113	20.03	0.01	0.33	0.00	0.79	0.01	648	513
114	21.29	0.07	0.96	0.07	1.97	0.09	646	602
115	21.15	0.07	0.84	0.04	1.63	0.08	643	582
116	21.52	0.05	1.00	0.09	1.69	0.10	642	610
117	21.08	0.06	0.82	0.04	1.78	0.07	641	589
118	21.26	0.05	1.02	0.08	1.79	0.09	634	636
119	21.91	0.13	0.74	0.06	1.30	0.14	633	550
120	20.83	0.03	1.62	0.17	3.14	0.17	624	482
121	22.18	0.21	0.76	0.06	1.20	0.22	603	555
122	21.83	0.16	0.75	0.07	1.53	0.17	602	583
123	21.54	0.07	0.78	0.08	1.50	0.10	596	625
124	21.61	0.11	0.92	0.09	1.68	0.14	590	619
125	21.00	0.04	0.73	0.02	1.43	0.05	585	549
126	21.08	0.03	0.82	0.05	1.73	0.06	584	598
127	20.01	0.01	0.98	0.01	2.03	0.01	583	570
128	21.30	0.07	0.87	0.05	1.65	0.08	581	584
129	21.83	0.16	0.68	0.06	1.33	0.17	574	611
130	21.29	0.07	0.91	0.09	2.10	0.11	572	548
131	22.08	0.20	1.08	0.10	1.60	0.22	570	595
132	21.52	0.08	0.98	0.06	1.63	0.10	563	577
133	21.05	0.05	0.82	0.04	1.51	0.06	562	549
134	21.05	0.05	0.62	0.02	1.18	0.05	560	568
135	22.20	0.21	0.85	0.09	1.36	0.23	556	535
136	20.26	0.01	0.92	0.04	1.97	0.02	550	589
137	20.48	0.02	1.08	0.03	2.25	0.03	546	560
138	21.26	0.07	1.46	0.15	2.69	0.16	538	468
139	21.35	0.08	0.82	0.08	1.78	0.11	536	590
140	21.03	0.03	1.10	0.05	1.85	0.06	535	629
141	20.06	0.02	0.93	0.03	1.77	0.02	535	621
142	21.03	0.04	0.92	0.04	1.92	0.05	533	520
143	18.46	0.00	0.91	0.00	1.77	0.00	533	612
144	21.00	0.05	0.71	0.04	1.51	0.06	532	537
145	22.70	0.29	0.84	0.13	0.89	0.31	532	576
146	20.49	0.02	0.76	0.02	1.59	0.03	527	607
147	20.81	0.04	0.76	0.03	1.66	0.05	522	557
148	22.07	0.17	0.66	0.05	1.02	0.18	520	644
149	21.65	0.13	0.75	0.04	1.18	0.14	518	602
150	21.27	0.07	0.89	0.03	1.54	0.08	516	619
151	21.89	0.13	0.49	0.15	1.13	0.19	515	464
152	21.33	0.05	0.73	0.04	1.50	0.06	514	523
153	21.46	0.07	0.89	0.08	1.68	0.11	515	500
154	21.42	0.09	1.02	0.13	2.04	0.15	515	444
155	21.37	0.06	0.78	0.05	1.52	0.08	514	508
156	20.90	0.02	0.34	0.03	0.78	0.02	509	421
157	21.27	0.08	0.71	0.05	1.54	1.10	508	508
158	20.94	0.03	1.00	0.03	2.06	0.04	505	388
159	22.01	0.15	0.62	0.10	1.30	0.17	505	619
160	21.31	0.04	0.90	0.04	1.49	0.06	503	651
161	21.38	0.05	0.84	0.07	1.81	0.08	502	328
162	21.04	0.04	0.74	0.04	1.66	0.05	501	357
163	21.03	0.06	0.82	0.03	1.77	0.07	501	537
164	17.34	0.00	1.05	0.00	2.31	0.00	495	437
165	20.45	0.01	1.13	0.03	2.35	0.03	494	561
166	21.89	0.14	0.81	0.08	1.20	0.16	493	663
167	22.56	0.35	0.23	0.12	0.81	0.35	491	523
168	21.06	0.06	0.92	0.04	1.77	0.07	491	354
169	20.74	0.04	1.10	0.05	2.51	0.06	491	376
170	20.83	0.04	1.14	0.07	2.92	0.08	490	294
171	21.54	0.08	0.58	0.08	1.45	0.10	488	569
172	22.69	0.39	0.79	0.19	1.28	0.41	488	596
173	22.13	0.16	0.66	0.06	0.96	0.17	487	460
174	20.67	0.02	1.06	0.05	2.19	0.05	486	326
175	21.32	0.07	1.06	0.07	1.86	0.10	485	413
176	20.47	0.01	1.63	0.06	3.19	0.06	484	628
177	21.05	0.02	0.81	0.03	1.67	0.03	484	513
178	21.65	0.10	0.82	0.06	1.42	0.11	481	537
179	20.97	0.04	1.08	...	2.18	...	480	557
180	21.23	0.09	0.86	0.06	1.72	0.11	478	301
181	21.48	0.10	1.02	0.06	2.03	0.12	477	648
182	21.94	0.09	1.23	0.22	2.18	0.23	477	588
183	20.95	0.03	0.75	0.02	1.51	0.03	476	436
184	19.83	0.01	0.82	0.03	1.72	0.02	475	623
185	20.60	0.03	0.92	0.06	2.05	0.05	474	368
186	20.55	0.01	0.88	0.04	1.94	0.04	471	379
187	20.60	0.03	1.48	0.07	3.12	0.07	464	378
188	19.70	0.01	1.13	0.01	2.42	0.01	463	353
189	20.52	0.02	1.20	...	2.63	...	462	534
190	20.98	0.03	1.00	...	2.11	...	458	600
191	21.23	0.05	0.85	0.04	1.60	0.06	457	510
192	19.46	0.01	0.95	0.01	1.81	0.01	455	682
193	20.80	0.02	0.60	0.02	1.41	0.02	454	536
194	20.94	0.05	0.74	0.02	1.58	0.06	452	351
195	21.14	0.05	1.58	0.30	2.77	0.30	450	451
196	21.75	0.09	0.77	0.05	1.49	0.10	448	475
197	22.46	0.26	0.85	0.20	1.50	0.32	447	566
198	17.79	0.00	0.81	0.01	1.70	0.00	444	653
199	21.55	0.06	1.16	0.24	2.35	0.24	443	445
200	21.12	0.05	0.49	0.03	1.35	0.06	438	445
201	20.91	0.04	0.68	0.04	1.57	0.06	433	382
202	20.51	0.02	0.75	0.03	1.74	0.03	431	547
203	21.62	0.08	0.64	0.08	1.71	0.10	422	594
204	19.93	0.01	0.82	0.01	1.76	0.01	422	296
205	20.65	0.03	1.02	0.05	2.57	0.05	422	394
206	20.70	0.02	1.10	0.04	2.23	0.04	421	512
207	19.97	0.01	0.90	0.01	1.67	0.01	416	535
208	21.26	0.08	0.71	0.04	1.40	0.09	413	436
209	20.58	0.03	0.74	...	1.72	...	413	364
210	21.28	0.06	0.77	0.03	1.79	0.07	410	417
211	20.73	0.02	0.85	0.03	1.93	0.04	408	395
212	20.70	0.03	1.02	0.03	2.26	0.04	407	505
213	19.96	0.01	0.38	0.01	1.00	0.01	406	329
214	21.76	0.11	0.68	0.05	1.23	0.12	405	457
215	21.34	0.05	0.89	0.06	1.82	0.07	404	580
216	20.55	0.02	0.80	0.01	1.68	0.03	402	402
217	21.73	0.15	0.79	0.05	1.47	0.15	402	486
218	21.21	0.06	0.91	0.10	2.03	0.11	402	448
219	20.64	0.02	1.08	0.04	2.27	0.05	402	149
220	21.67	0.11	0.92	0.18	2.11	0.20	399	460
221	20.86	0.04	0.95	0.02	1.85	0.04	397	406
222	22.23	0.27	0.72	0.09	1.20	0.27	391	595
223	21.71	0.12	0.58	0.04	1.07	0.12	389	483
224	20.91	0.05	0.82	0.02	1.72	0.05	388	316
225	19.94	0.01	1.21	0.03	2.69	0.03	387	208
226	21.54	0.10	0.95	0.06	1.91	0.11	387	391
227	21.03	0.05	0.63	0.02	1.37	0.05	386	252
228	20.72	0.02	0.79	0.01	1.62	0.02	381	319
229	20.88	0.03	1.62	0.12	2.75	0.12	377	525
230	21.64	0.08	0.61	0.05	1.22	0.09	377	337
231	21.59	0.13	0.64	0.05	1.37	0.14	374	184
232	22.61	0.32	0.76	0.18	1.02	0.36	373	500
233	21.46	0.08	1.01	0.06	1.77	0.10	373	494

TABLE 2—*Continued*

No. (1)	I (2)	$\pm$[a] (3)	$V-R$ (4)	$\pm$[a] (5)	$V-I$ (6)	$\pm$[a] (7)	x (8)	y (9)
234	21.16	0.06	0.94	0.06	1.84	0.08	372	302
235	21.01	0.04	1.25	0.06	2.49	0.07	372	480
236	21.19	0.08	0.67	0.05	1.70	0.09	370	448
237	21.75	0.14	0.92	0.12	1.87	0.18	370	519
238	21.07	0.04	0.88	0.03	1.87	0.05	370	255
239	21.81	0.11	0.62	0.08	1.28	0.13	368	512
240	21.31	0.06	0.96	0.05	1.97	0.07	368	592
241	21.30	0.07	0.80	0.06	1.74	0.10	367	327
242	21.59	0.10	0.64	0.05	1.34	0.10	368	189
243	20.83	0.04	0.59	0.02	1.41	0.04	365	457
244	21.26	0.05	0.78	0.04	1.54	0.06	364	259
245	20.73	0.02	0.92	0.03	1.88	0.03	361	311
246	20.96	0.04	1.21	0.12	2.53	0.13	361	461
247	21.16	0.07	0.88	0.04	1.74	0.08	360	234
248	22.15	0.21	0.62	0.09	1.23	0.22	357	624
249	22.64	...	0.93	0.27	1.55	...	356	611
250	20.61	0.02	1.36	0.11	2.96	0.11	355	509
251	21.64	0.10	0.76	0.06	1.44	0.12	354	405
252	20.64	0.04	0.78	0.03	1.79	0.05	350	576
253	21.56	0.09	0.59	0.04	1.11	0.09	350	629
254	20.45	0.01	1.44	0.08	3.09	0.08	350	161
255	19.50	0.00	1.16	0.01	2.18	0.01	350	227
256	20.80	0.03	0.93	0.06	2.00	0.06	349	258
257	21.78	0.12	0.59	0.04	1.32	0.12	348	448
258	20.98	0.04	0.72	0.02	1.83	0.05	346	470
259	21.67	0.13	0.66	0.06	1.23	0.14	346	476
260	20.83	0.04	1.25	0.08	2.70	0.08	342	488
261	21.54	0.11	0.78	0.04	1.40	0.12	340	608
262	21.25	0.09	...	...	1.60	0.10	337	198
263	21.81	0.17	0.67	0.11	1.67	0.19	337	406
264	21.42	0.07	0.67	0.04	1.45	0.08	337	465
265	21.39	0.07	0.61	0.05	1.32	0.08	333	578
266	22.22	...	0.63	0.07	1.04	...	332	487
267	21.50	0.08	0.74	0.03	1.29	0.08	332	319
268	18.32	0.00	1.41	0.00	3.08	0.00	331	362
269	21.26	0.03	0.66	0.06	1.83	0.06	327	517
270	21.79	0.13	0.65	0.08	1.45	0.15	327	181
271	21.08	0.03	0.75	0.02	1.28	0.04	326	346
272	20.82	0.03	0.78	0.02	1.68	0.04	320	335
273	21.82	0.12	1.00	0.21	2.13	0.23	319	186
274	22.10	0.27	0.84	0.06	1.19	0.27	318	379
275	20.22	0.01	1.17	0.03	2.53	0.03	316	273
276	21.32	0.07	1.68	0.38	3.43	0.38	314	542
277	21.33	0.06	0.76	0.07	1.64	0.09	312	498
278	20.52	0.03	0.85	0.02	1.70	0.03	312	411
279	21.11	0.03	1.03	0.10	2.28	0.11	312	280
280	20.69	0.02	0.76	0.01	1.49	0.02	310	288
281	20.44	0.01	0.89	0.01	2.00	0.02	305	324
282	21.51	0.06	0.63	0.06	1.36	0.08	305	384
283	21.47	0.06	0.74	0.03	1.59	0.07	302	497
284	21.47	0.10	1.30	0.13	2.16	0.16	302	344
285	23.24	0.46	1.12	0.51	2.00	0.62	301	400
286	20.79	0.02	0.92	0.03	1.77	0.03	301	282
287	20.30	0.01	0.82	0.01	1.63	0.01	299	354
288	21.60	0.06	0.85	0.08	1.77	0.09	295	646
289	21.18	0.05	0.82	0.04	1.54	0.06	293	183
290	21.61	0.06	0.68	0.03	1.14	0.07	292	220
291	21.06	0.02	0.72	0.03	1.57	0.03	291	469
292	21.03	0.04	0.80	0.03	1.45	0.05	290	611
293	21.33	0.05	0.59	0.03	1.35	0.05	290	340
294	20.56	0.02	1.02	0.02	2.23	0.02	287	396
295	20.59	0.02	0.99	0.04	2.27	0.04	287	527
296	21.68	0.08	0.63	0.03	1.17	0.09	282	322
297	19.83	0.01	1.10	0.01	2.42	0.01	281	538
298	21.69	...	0.90	0.09	1.62	...	281	296
299	21.46	0.11	0.55	0.04	1.23	0.11	277	306
300	21.57	0.12	...	...	1.87	0.14	276	416
301	20.93	0.03	0.91	0.03	1.93	0.04	276	213
302	21.20	0.05	0.96	0.05	1.80	0.07	275	349
303	21.31	0.07	0.67	0.02	1.31	0.07	275	335
304	21.40	0.06	0.63	0.04	1.42	0.06	275	296
305	20.14	0.01	1.45	0.08	3.05	0.08	274	462
306	20.97	0.02	...	...	1.81	0.06	271	193
307	17.37	0.00	0.45	0.02	1.09	0.01	267	508
308	21.16	0.04	0.84	0.03	1.63	0.05	264	211
309	21.23	0.05	0.74	0.05	1.36	0.06	262	556
310	22.94	0.40	0.63	0.17	0.79	0.42	261	357
311	20.91	0.03	0.92	0.02	1.86	0.04	257	441
312	22.23	...	0.13	0.04	0.21	...	256	258
313	21.49	0.10	1.32	0.15	2.38	0.18	255	448
314	21.50	0.08	0.90	0.07	1.66	0.10	255	407
315	18.56	0.00	1.03	0.00	2.15	0.00	255	600
316	21.77	...	0.64	0.06	1.25	...	251	299
317	21.83	0.14	0.73	0.05	1.24	0.15	251	331
318	21.04	0.02	0.82	0.03	1.59	0.03	251	579
319	21.43	0.05	0.92	0.06	1.51	0.07	244	239
320	21.70	0.14	0.98	0.10	1.76	0.17	241	245
321	22.17	0.22	0.87	0.13	1.35	0.25	240	280
322	21.08	0.06	1.26	0.06	2.33	0.08	240	387
323	21.42	0.09	0.87	0.03	1.54	0.09	239	323
324	20.41	0.01	1.17	0.04	2.45	0.04	238	273
325	21.42	0.07	0.91	0.03	1.69	0.07	233	201
326	20.98	0.04	1.04	0.09	2.23	0.10	231	528
327	20.48	0.02	0.84	0.02	1.63	0.03	230	470
328	21.61	0.09	0.84	0.06	1.47	0.10	229	545
329	21.55	0.06	0.76	0.02	1.15	0.06	226	240
330	21.45	0.05	0.72	0.05	1.39	0.07	223	199
331	21.02	0.03	1.05	0.14	2.87	0.13	223	478
332	21.43	0.06	1.00	0.10	2.01	0.11	222	327
333	22.94	0.44	1.06	0.16	0.87	0.46	217	241
334	21.18	0.05	0.94	0.07	1.94	0.08	217	518
335	21.10	0.03	1.16	0.04	1.96	0.05	216	587
336	20.27	0.01	1.05	0.03	2.12	0.03	216	414
337	19.73	0.00	0.54	0.00	1.01	0.00	216	319
338	20.74	0.02	0.92	0.02	1.85	0.02	213	500
339	21.65	0.07	1.01	0.07	1.67	0.10	211	208
340	20.97	0.04	1.17	0.05	2.27	0.06	210	293
341	20.75	0.02	1.07	0.08	2.36	0.08	207	489
342	21.78	0.07	0.75	0.06	1.39	0.09	206	371
343	21.78	0.13	1.08	0.12	1.54	0.18	205	323
344	19.37	0.00	1.05	0.01	2.21	0.01	204	525
345	21.19	0.04	0.80	0.03	1.38	0.05	202	334
346	21.32	0.06	0.81	0.01	1.22	0.06	202	246
347	21.08	0.04	0.92	0.04	1.62	0.06	201	205
348	21.26	0.05	0.82	0.03	1.49	0.06	194	266
349	23.09	0.43	0.59	0.14	0.37	0.45	194	197
350	21.84	0.18	0.78	0.08	1.57	0.20	188	283
351	21.46	0.05	0.92	0.07	1.72	0.08	183	342
352	21.75	0.13	0.95	0.07	1.39	0.15	183	385
353	20.60	0.03	1.15	0.03	2.31	0.04	179	379
354	21.97	0.15	1.08	0.14	1.82	0.20	177	288
355	21.76	0.08	0.95	0.10	1.76	0.12	177	334
356	19.79	0.01	0.40	0.00	0.85	0.01	177	119
357	20.17	0.01	0.81	0.01	1.63	0.01	175	637
358	21.25	0.07	0.80	0.04	1.52	0.08	169	651
359	20.55	0.01	0.96	0.03	2.10	0.03	167	231
360	21.17	0.04	1.03	0.06	1.92	0.07	167	290
361	22.30	0.20	0.66	0.07	0.98	0.21	163	373
362	20.40	0.02	0.91	0.03	2.06	0.03	163	497
363	17.22	0.00	1.14	0.00	2.43	0.00	159	584
364	22.17	0.15	0.92	0.10	1.15	0.18	158	270
365	21.88	0.09	0.91	0.09	1.42	0.13	157	411
366	21.38	0.08	0.61	0.07	1.49	0.10	154	665
367	21.21	0.05	1.03	0.04	1.83	0.07	154	376
368	22.29	0.19	0.74	0.08	0.99	0.20	154	321
369	20.89	0.03	0.85	0.03	1.73	0.04	152	515
370	21.79	0.10	1.03	0.11	1.53	0.15	151	307
371	20.49	0.01	1.25	0.05	2.55	0.05	148	562

TABLE 2—*Continued*

No. (1)	I (2)	±[a] (3)	$V-R$ (4)	±[a] (5)	$V-I$ (6)	±[a] (7)	x (8)	y (9)
372	21.26	0.05	0.77	0.04	1.42	0.06	148	245
373	20.55	0.01	1.15	0.04	2.18	0.05	147	459
374	21.06	0.04	0.81	0.02	1.46	0.05	141	380
375	20.48	0.01	2.59	0.41	4.67	0.41	140	599
376	20.70	0.02	0.86	0.02	1.65	0.03	139	330
377	20.72	0.03	1.05	0.03	2.04	0.04	135	268
378	22.01	0.10	0.64	0.08	1.04	0.12	135	288
379	21.67	0.13	0.76	0.07	1.44	0.14	133	210
380	21.86	0.11	0.82	0.08	1.36	0.13	130	239
381	20.99	0.05	0.86	0.03	1.67	0.05	130	275
382	20.78	0.04	0.53	0.01	0.96	0.04	129	398
383	19.39	0.02	0.93	0.01	1.82	0.02	127	219
384	21.81	0.10	0.61	0.08	1.33	0.11	126	303
385	21.20	0.04	1.00	0.05	1.74	0.06	123	398
386	20.88	0.03	...	...	1.89	0.04	119	262
387	21.27	0.06	...	...	1.35	0.07	116	400
388	18.17	0.00	...	...	2.36	0.00	108	612

[a] These are formal internal errors: Estimated total external errors are of order 2–3 times larger.

$V-I$ color at $M_I = -3$ and interpolate the loci of globular clusters. For 87 stars between $I = 21.1$ and 21.6, we obtain $\langle V-I \rangle = 1.67$ with $\sigma(V-I) = 0.31$ after rejection of a single 3 σ deviate. The mean value of I for these stars is 21.34. Uncertainty in the distance modulus and reddening would increase the uncertainty in $\langle V-I \rangle$ to ± 0.13 mag.

Before we can use this value, however, we must consider possible sources of systematic error. The first of these is contamination by foreground and background sources. From the off-galaxy field in Paper I we estimate that approximately 11% of the 87 stars fall into this category. The mean color of these stars (rejecting these with $V-I > 2.7$) is 1.84. Second, there is the problem of the presence of M31 halo stars. We can estimate the degree of contamination from surface photometry of M31 by de Vaucouleurs (1958) and of NGC 205 by Hodge (1973). Slightly extrapolating their data, we find $B = 28.0$ mag arcsec^{-2} for the M31 halo and $V = 25.0$ mag arcsec^{-2} in our field. The mean color of the M31 halo in this vicinity is $B-V = 0.86$ (see Baum and Schwarzschild 1955). Assuming similarity in their stellar populations, we estimate that 13% of the stars on the giant branch shown in Figure 4 actually belong to M31. Interpolating the integrated color between those of 47 Tuc ($[M/H] = 0.8$) and the mean Galactic globular cluster ($[M/H] = -1.6$), using data from Harris and Racine (1979), we estimate a mean color for these M31 stars of 1.44 in $(V-I)_0$. These two corrections cancel in the calculation of $\langle V-I \rangle$ for the NGC 205 giant branch at $M_I = -3$.

Finally, we consider the completeness of the data for $I = 21.1$–21.6. Although it is possible that the paucity of stars with $V > 24.0$ and $I < 22$ (the dashed line in Fig. 4) could result from an upper bound to the metallicity of NGC 205, it seems more likely that this is a completeness limit for the V magnitudes. Without a detailed analysis of the selection function, it is impossible to estimate the bias caused by incompleteness. We note that its effect is mainly to reduce the number of stars redward of the 47 Tuc locus in Figure 4, and therefore to underestimate both the metallicity and metallicity dispersion in NGC 205. Whether this bias is significant depends on whether the incompleteness in V is a steep or shallow

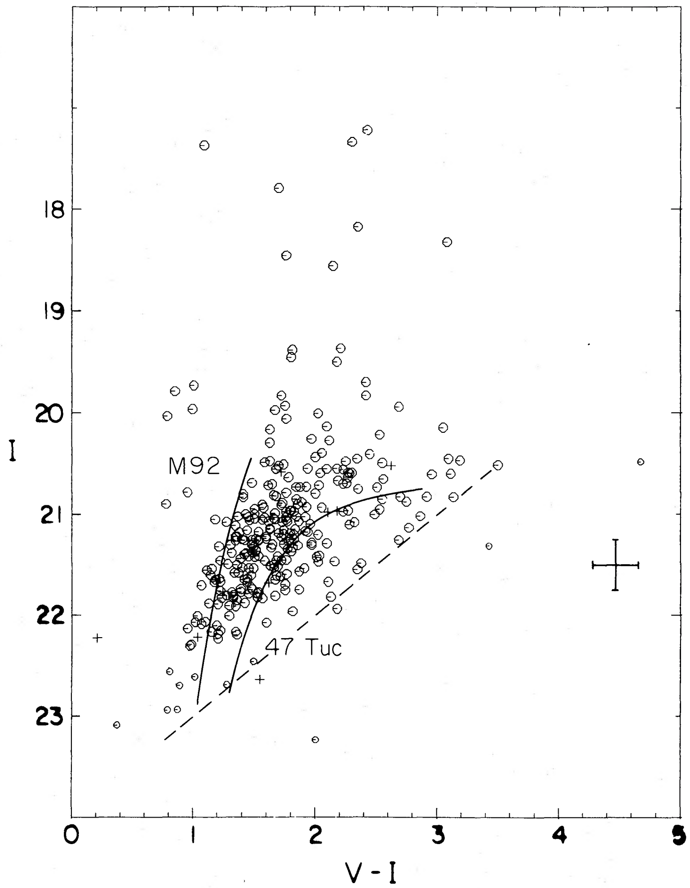

FIG. 4.—The color-magnitude diagram for NGC 205. The symbols are the same as in Fig. 3. Also shown are the mean giant branches of the globular clusters M92 and 47 Tuc, connected to the distance and extinction of NGC 205. The diagonal dashed line is at $V = 24$ mag, near our estimated completeness limit. All or most stars brighter than $I = 20.4$ are field stars; most stars fainter than this belong to the giant branch of NGC 205. The brightness of the tip of the giant branch gives an improved distance modulus of 24.3 mag. The large color dispersion, with many stars redder than the 47 Tuc line, is real and is not seen in a parallel study of NGC 147. This field does not show the young and intermediate-age stellar population suggested near the center of NGC 205.

function of V magnitude. The best answer to this question is deeper V imaging.

With only a reddening correction applied, we obtain $\langle V-I \rangle_0 \geq 1.60 \pm 0.13$, which corresponds to a mean metallicity of -0.85 ± 0.2 on the globular cluster scale of Paper I. Following the discussion of photometric errors in § II, we note that a metallicity dispersion has been detected in NGC 205 and estimate that $\sigma([M/H]) \geq 0.5$ dex. Both the mean metallicity and the dispersion are larger than in NGC 147.

IV. THE TIP OF THE GIANT BRANCH

The luminosity function in the NGC 205 field is compared with that in the off-galaxy field in Figure 5. The abrupt break in the luminosity function slope at $I = 20.4$ can be identified with the tip of the first giant branch in Galactic globular clusters, since, with the adopted distance modulus and

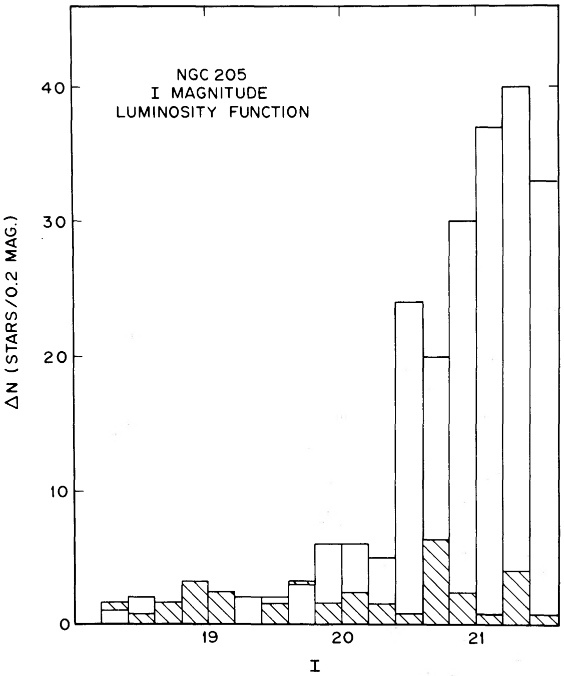

FIG. 5.—The differential luminosity function in NGC 205. Stars were counted in intervals of 0.2I mag. The hatched histogram which is superposed shows the luminosity function of a corresponding control field away from the galaxy (and farther from M31).

reddening and appropriate bolometric correction,[3] it occurs at $M_{\rm bol} = -3.5 \pm 0.3$.

We can employ the apparent magnitude of this break in the luminosity function, together with a new calibration of the peak bolometric magnitude at the tip of the first giant branch (Frogel, Cohen, and Persson 1983, eq. [4]), to improve the distance modulus for NGC 205. Assuming $\langle[\mathrm{Fe/H}]\rangle = -0.85 \pm 0.2$, and $\langle V-I \rangle = 2.0 \pm 0.5$, we obtain $(m-M)_I = 24.43 \pm 0.15$. If we were to hypothesize an age difference between NGC 205 and Galactic globular clusters of ± 5 Gyr and a helium abundance difference of $\delta Y = \pm 0.05$, or if we employed the dashed line in Figure 6 of Frogel, Cohen, and Persson (1983) in place of the solid one, the resultant uncertainty would increase to 0.2 mag. Corrected for reddening, we estimate a distance modulus for NGC 205 of $(m-M)_0 = 24.3 \pm 0.2$. The revised distance modulus changes our derived mean metallicity to $[M/H] = -0.9 \pm 0.2$.

We also note in Figure 5 an apparent excess of stars in the NGC 205 field just below the break ($19.8 < I < 20.4$). Several possibilities come to mind concerning the nature of these stars:

1. They could be variable stars observed in the luminous phase of their cycle. However, variable stars with $V - I_K < 2$ (i.e., $V - I_c < 2.14$) seem to be rare in the globular cluster sample of Lloyd-Evans and Menzies (1977), and the I amplitude of such stars is small (Eggen 1972). Long-period variable stars such as V3 in 47 Tuc become bluer as they brighten (Eggen 1972), but not to the extent seen in Figure 4.

2. They could be foreground stars. There are 17 stars in this magnitude interval, where seven would have been expected from the off-galaxy field. It would not be statistically unlikely that most of the observed stars are foreground objects.

3. They could be asymptotic giant branch (AGB) stars. In the Galaxy, however, metal-poor globular clusters tend not to show AGB stars brighter than the red giant tip, and metal-rich clusters contain rather redder (and variable) AGB stars.

4. They could be, but are probably not, due to photometric error. The estimated photometric errors at $I = 20.4$ are smaller than 0.1 mag.

We cannot distinguish between these possibilities with the present small set of observations. Clearly, however, the search for long-period variable stars in NGC 205 may be fruitful, given the metal abundance we find in this galaxy.

Finally, we comment on the absence in this NGC 205 field of the extended giant branch seen in the dwarf spheroidal satellites of the Galaxy. If Fornax or Carina were moved to the distance of M31, we would see a string of luminous AGB stars extending from the red giant tip to an I magnitude of 18.3 in the first case or 19.4 in the second case and colors of $V - I > 3$ (Aaronson and Mould 1980; Mould *et al.* 1982). If, as in Fornax, 10% of the stellar population in this field were of intermediate age (2–8 Gyr), then it could be shown, as in Paper I, that approximately four stars per magnitude would be expected between 18.3 and 19.4 I magnitude in the NGC 205 field in excess of the off-galaxy field. This can be ruled out from Figure 5. Such strict limits could not, however, be put on an *older* intermediate-age population (as seen in Carina; see Mould and Aaronson 1983), because of the marginally significant excess of stars in this field between $I = 19.4$ and the red giant tip.

V. COMPARISON WITH OTHER DWARF ELLIPTICAL GALAXIES

A comparison of the outer parts of NGC 205 and the faintest of the M31 E companions, NGC 147, reveals considerable similarities. Both are old stellar populations with upper limits of 10% on the mass of an intermediate-age component. The outer parts of NGC 205 have a marginally significant higher mean metallicity than those of NGC 147 and probably have a larger dispersion in metallicity. Since the absolute V magnitude of NGC 205 is -16.5, 1.4 mag brighter than NGC 147, however, the former difference would be expected on the basis of the mass-metallicity relation discussed in Paper I. Integrated UBV colors have been measured off-center for these galaxies by Sandage (1972). From the calibration of integrated colors by Aaronson *et al.* (1978), the metallicity difference of 0.3 ± 0.3 would correspond to $\Delta(U-V) = 0.12 \pm 0.12$. Sandage's photometry corrected for reddening has a mean value of 0.96 for NGC 205 and $(U-V)_0 = 0.94$ for NGC 147.

The most striking difference between NGC 205 and NGC 147 is the presence in the former case of luminous blue stars in the central 1'.5. Our results are *not* inconsistent with the hypothesis of Gallagher and Hunter (1981) that this star formation is fueled by gas recycled from the dominant old stellar population. In this case, however, the gas would

[3] The bolometric correction to the I magnitude as a function of $(V-I)_0$ has been redetermined (cf. Paper I) using data from the (V, $V-I$) photometry of Lloyd-Evans (1983) and the infrared photometry of Frogel, Persson, and Cohen (1983). From 96 stars in seven globular clusters with small reddenings, the bolometric correction to the I magnitude is found to be $\mathrm{BC}_I = 0.906 - 0.246(V-I)_0$. This relation differs from that given in Paper I by more than 0.1 mag only for $(V-I)_0 > 2.2$.

need to flow to the center before new star formation occurred. Some loss of gas from the exterior is also possible. According to $r^{1/4}$ law models by Young (1976), the escape velocity at the radius of our field in NGC 205 has fallen to less than half its value in the center of the potential and is comparable to the escape velocity in the larger Galactic globular clusters. Integrated photometry is also useful in constraining the star formation rate in NGC 205. Unless this galaxy has a quite unusual inverted metallicity gradient, the compilation of photometry by Hodge (1973) requires that the integrated blue light from young and intermediate-age stars must be comparable to the output from the old stellar population. A simplistic two-component model for the central 1'.5 has one old component with the colors of the outer parts and another whose $B-V$ colors are those of continuous star formation from 15 Gyr ago (Larson and Tinsley 1978). The required star formation rate is $3 \times 10^{-4}\ M_\odot\ \mathrm{yr}^{-1}$, which agrees with the calculation by Gallagher and Hunter based on star counts. With the recycling rates adopted by these authors it is clear that some inflow of gas from regions outside this central volume would help to maintain equilibrium.

A recent comparison of the broad range of elliptical galaxies (Sandage 1983) has stressed the strong continuity in properties over a luminosity range of 10^6. A number of details, however, distinguish the dwarf ellipticals in the present study from the fainter dwarf spheroidal satellites of the Galaxy. The present work shows that they share with the dwarf spheroidals a finite metallicity dispersion (indicating a history of star formation of more than one generation). They differ in that some of the dwarf spheroidals have formed a *significant* ($\geq 10\%$) fraction of their stellar mass in more recent times (Mould and Aaronson 1983; Seitzer 1982; Aaronson and Mould 1980). Continuity between dwarf and giant ellipticals is also evident in a mass-metallicity relation (see Paper I and Caldwell 1983), but it is noteworthy that gE galaxies reverse the trend of increasing median surface brightness with increasing luminosity (Sandage 1983). Further study will be required before we know if *one* formation theory will serve for all elliptical galaxies.

VI. SUMMARY

A color-magnitude diagram for a field 2 kpc out on the major axis reveals the first two magnitudes of the giant branch in NGC 205. We find: (1) If the distance of the galaxy is that of M31, the stellar population in this field is overwhelmingly old. Less than 10% of the integrated luminosity at this radius comes from stars aged between 2 and 8 Gyr. If star formation in NGC 205 is a recurring phenomenon, it is confined to the interior of the galaxy. (2) If the stellar population of NGC 205 is as old as Galactic globular clusters, its distance modulus is 24.3 ± 0.2. (3) The location of the giant branch corresponds to a *mean* metallicity $[M/H] \geq -0.9 \pm 0.2$. (4) A metallicity *dispersion* of $\sigma[M/H] \geq 0.5$ dex has been determined. The color distribution at a given luminosity appears to be positively skewed. Some stars almost as metal poor as those of M92 are indicated, and some considerably more metal rich than those of 47 Tuc.

Many members of the Space Telescope Wide Camera Team made direct contributions to this project, and we wish to express our gratitude to them. Special thanks go to Bill Ditsler at KPNO for assistance with the setup and to John Hoessel for supplying HERCULES. This work was partially supported by a NASA grant to the Carnegie Institution of Washington, and NSF grant AST 8306139.

REFERENCES

Aaronson, M., Cohen, J. G., Mould, J. R., and Malkan, M. 1978, *Ap. J.*, **223**, 824.
Aaronson, M., and Mould, J. R. 1980, *Ap. J.*, **240**, 804.
Baade, W. 1944, *Ap. J.*, **100**, 137.
———. 1951, *Pub. Univ. Mich. Obs.*, **10**, 7.
Baum, W. A., and Schwarzschild, M. 1955, *A.J.*, **60**, 247.
Burstein, D., and Heiles, C. 1982, *A.J.*, **87**, 1165.
Caldwell, N. 1983, *A.J.*, **88**, 804.
Cousins, A. W. J. 1976*a*, *Mem. R.A.S.*, **81**, 25.
———. 1976*b*, *M.N.A.S. So. Africa*, **35**, 70.
de Vaucouleurs, G. 1958, *Ap. J.*, **128**, 465.
Eggen, O. J. 1972, *Ap. J.*, **172**, 639.
Frogel, J. A., Cohen, J. G., and Persson, S. E. 1983, *Ap. J.*, **275**, 773.
Frogel, J. A., Persson, S. E., and Cohen, J. G. 1983, *Ap. J. Suppl.*, **53**, 713.
Gallagher, J. S., and Hunter, D. A. 1981, *A.J.*, **86**, 1312.
Gallagher, J. S., and Mould, J. R. 1981, *Ap. J.* (*Letters*), **244**, L3.
Harris, W. E., and Racine, R. 1979, *Ann. Rev. Astr. Ap.*, **17**, 241.
Hodge, P. W. 1973, *Ap. J.*, **182**, 671.
Johnson, D. W., and Gottesman, S. T. 1982, *Bull. AAS*, **13**, 893.
Larson, R., and Tinsley, B. M. 1978, *Ap. J.*, **219**, 46.
Lloyd-Evans, T. 1983, preprint.
Lloyd-Evans, T., and Menzies, J. W. 1977, *M.N.R.A.S.*, **178**, 163.
Mould, J. R., and Aaronson, M. 1983, *Ap. J.*, **273**, 530.
Mould, J. R., Cannon, R. D., Aaronson, M., and Frogel, J. A. 1982, *Ap. J.*, **254**, 500.
Mould, J. R., Kristian, J., and Da Costa, G. S. 1983, *Ap. J.*, **270**, 471 (Paper I).
Sandage, A. R. 1961, *The Hubble Atlas of Galaxies* (Carnegie Institution of Washington Pub. 618).
———. 1972, *Ap. J.*, **176**, 21.
———. 1983, *Carnegie Yrb.*, **81**, 623.
Seitzer, P. 1982, private communication.
Unwin, S. C. 1980, *M.N.R.A.S.*, **190**, 551.
Young, P. J. 1976, *A.J.*, **81**, 807.

GARY S. DA COSTA: Department of Astronomy, Yale University, P.O. Box 6666, New Haven, CT 06511

JEROME KRISTIAN: Mount Wilson and Las Campanas Observatories, 813 Santa Barbara Street, Pasadena, CA 91101

JEREMY R. MOULD: Caltech, 105–24, Pasadena, CA 91125